

In silico analysis of piRNAs in retina reveals potential targets in intracellular transport and
retinal degeneration

Suganya Sivagurunathan^{a, b†}, Nagesh Srikakulam^{c†}, Jayamuruga Pandian Arunachalam^d,
Gopal Pandi^c, Subbulakshmi Chidambaram^{a, e*}

^aRS Mehta Jain Department of Biochemistry and Cell Biology, Vision Research Foundation,
Chennai, India.

^bSchool of Chemical and Biotechnology, SASTRA University, Thanjavur, India.

^cDepartment of Plant Biotechnology, School of Biotechnology, Madurai Kamaraj
University, Madurai 625021, Tamil Nadu, India.

^dCentral Inter-Disciplinary Research Facility (CIDRF), Sri Balaji Vidyapeeth University,
Mahatma Gandhi Medical College and Research Institute Campus, Pondicherry, India.

^eDepartment of Biochemistry and Molecular Biology, Pondicherry University, Puducherry,
India.

[†]Both authors contributed equally to this work

*Email ID – csubbulakshmi@gmail.com

Abstract

Long considered to be active only in germline, PIWI/piRNA pathway is now known to play significant role in somatic cells, especially neurons. Nonetheless, so far there is no evidence for the presence of piRNAs in the neurosensory retina. In this study, we have uncovered 102 piRNAs in human retina and retinal pigment epithelium (RPE) by analysing RNA-seq data. The identified piRNAs were enriched with three motifs predicted to be involved in rRNA processing and sensory perception. Further, expression of piRNAs in donor eyes were assessed by qRT-PCR. Loss of piRNAs in HIWI2 knockdown ARPE19 cells downregulated targets implicated in intracellular transport (SNAREs and *Rabs*), circadian clock (*TIMELESS*) and retinal degeneration (*LRPAP1* and *RPGRIP1*). Moreover, piRNAs were dysregulated under oxidative stress indicating their potential role in retinal pathology. Intriguingly, computational analysis revealed complete and partial seed sequence similarity between piR-62011 and sensory organ specific miR-183/96/182 cluster. Furthermore, the expression of retina enriched piR-62011 positively correlated with miR-182 in HIWI2 silenced Y79 cells. Thus, our data provides an evidence for the expression of piRNAs in human retina and RPE. Collectively, our work demonstrates that piRNAs dynamically regulate distinct molecular events in the maintenance of retinal homeostasis.

Introduction

Retina, a neurosensory tissue of the eye, is developed from inner layer of optic cup regulated by eye field specific transcription factors (EFTF) whereas Retinal Pigment Epithelium (RPE) develops from outer layer of optic cup. Photoreceptors of the retina converts photons of light into electrical impulses where the crosstalk with RPE is necessary. Recent studies have indicated the involvement of non-coding RNAs in eye development plausibly by targeting the EFTF¹. Besides their role in development, the importance of non-coding RNAs in visual function was confirmed when the depletion of miRNAs resulted in loss of outer segments of cone photoreceptors causing reduced light response². Further, non-coding RNAs are also linked with retinal pathologies and are suggested to be novel targets for therapy³.

piRNAs are a group of small noncoding RNAs which bind with PIWI subclade of Argonaute family proteins⁴⁻⁶. They are 24 – 32 nucleotides (nt) long, methylated at their 3' ends^{7,8} and are produced by a pathway independent of Dicer, making them distinct from other small noncoding RNAs. These group of RNAs are essential for maintaining the genomic integrity in germline cells by repressing the transposable elements⁹. Initially, it was thought to be restricted to germ cells, however, recent reports indicate their presence in various somatic tissues^{10,11} and cancer cells¹²⁻¹⁴. In addition, altered expression of piRNAs is observed during various pathological conditions like cardiac hypertrophy¹⁵ and liver regeneration¹⁰ in rats. Thus, growing evidence on the role of piRNAs in various non-germline tissues underscores the need to explore their importance in specific somatic cells as well.

Recent years has seen a surge of research findings on the existence of piRNAs in neurons. Initially, Lee *et al* has suggested roles for piRNAs in modulating the dendritic spine development in mouse hippocampal neurons¹⁶. In addition, altered expression of piRNAs were reported in rat brain after transient focal Ischemia¹⁷. Interestingly, a mechanistic role for

piRNAs in neurons has been demonstrated by Rajasethupathy *et al* where PIWI/piRNA complexes in *Aplysia* enhanced memory-related synaptic plasticity through epigenetic regulation of CREB2¹⁸. Recently, piRNAs have shown to attenuate the axonal regeneration of adult sensory neurons in rats¹⁹. Moreover, piRNAs are deregulated in Alzheimer's disease (AD) and are known to affect the disease associated pathways²⁰. Nevertheless, there is no study on the presence and role of PIWI-interacting RNAs (piRNAs) in retina.

In our recent reports, we have shown that PIWI-like proteins are expressed in human retina and HIWI2 (PIWIL4) regulates tight junctions in maintaining the integrity of RPE²¹. HIWI2 also alters the expression of OTX2, an eye field specification marker in human retinoblastoma cells²². The presence of PIWI-like proteins in retina strongly implies the existence of piRNAs. Therefore, we investigated the expression and role of piRNAs in retina and RPE. The present study identified 102 piRNAs by computational analysis of RNA-seq data obtained from human retina and RPE tissues. Additionally, novel targets of piRNAs in multiple molecular processes have been validated. Our data presents new insights into the functions of piRNAs in retina and RPE.

Results

Expression of piRNAs in human retina and RPE

We examined whether piRNAs are expressed in retina and RPE by analysing the small RNA sequencing data retrieved from ArrayExpress (Accession ID: E-MTAB-3792)²³. It consisted of 16 samples of human retina and 2 samples of RPE. The small RNA sequences were checked for their quality and the reads were mapped with the annotated small RNAs (tRNA, snRNA, snoRNA, miRNA, rRNA, mtRNA). The mapped reads were discarded to filter out the known small RNAs and the unmapped reads were aligned to the human genome. The resulting reads were considered as potential piRNA candidates and were mapped with the sequences of

piRNAs downloaded from piRNAQuest²⁴ (Fig.1). Interestingly, we observed 102 piRNAs with tags per million (TPM) values > 1. piRNAs that were expressed in retina and RPE are listed in Table S1. A heatmap on the expression of the identified piRNAs indicated that piR-31068, piR-35982, piR-35284 were in abundance in both the tissues analysed. Interestingly, piR-62011, piR-36743 and piR-36742 were highly expressed only in retina. Similarly, the expression of piR-35411, piR-35412, piR-35413, piR-31104 and piR-31103 were higher only in RPE tissue (Fig. 2a & b). Together, the results showed that piRNAs were expressed in ocular tissues and indeed differential expression of piRNAs were observed between retina and RPE.

Tissue enriched piRNAs

Having observed the piRNAs in ocular tissues, we next investigated whether the identified piRNAs are tissue specific. To this end, our data was compared with the piRNAs so far reported in human brain, cardiac progenitors and cardiac fibroblasts, ovary and testis^{20,25-27}. We observed 4 piRNAs (piR-30855, piR-34535, piR-44719 and piR-61647) to be expressed only in retina and RPE. All the analysed tissues shared 5 piRNAs (piR-33382, piR-33468, piR-35284, piR-35413 and piR-36225) in common. Moreover, 3 piRNAs (piR-32376, piR-43771 and piR-62011) were found to be commonly present in retina, RPE and testis. However, piR-62011 is abundantly expressed in retina (TPM value - 112874) when RPE is considered (TPM value - 1003) (Fig 2b). Notably, around 75% of the piRNAs in the retina/RPE tissues matched with the piRNAs in brain, followed by 72% with ovary. In contrast, piRNAs of ocular tissues showed only 35% and 34% match with testis and cardiomyocytes (cardiac progenitors and cardiac fibroblasts) respectively (Fig. 2c). Thus, a significant overlap was found amongst piRNAs expressed in human brain and retina/RPE; and piR-62011 appeared to be a retina enriched piRNA.

Genomic origin of piRNAs

piRNAs are shown to originate originally from the transposon sequences. The origin of the identified piRNAs indicated that majority of them mapped to tRNA family repeats, especially to tRNAs Val and Gly followed by Ala. This is in accordance with the earlier report on somatic piRNAs derived from the tRNA fragments²⁸. Moreover, protein coding genes were also known to be a source of piRNAs²⁹ and likewise our data specified 28 protein coding genes as origin for a set of piRNAs. Besides, 20 of the piRNAs originated from SNORD gene family which encodes small nucleolar RNAs (snoRNA). Recently, small nucleolar RNAs were reported to be precursor of piRNA³⁰. Strikingly, the retina enriched piR-62011 had its origin in the 3' UTR of miR-182 (Fig. 3a & b, Table S2).

Unlike the piRNAs expressed in germline cells, somatic piRNAs are reported to map 'piRNA clusters' to a lesser extent³¹. In order to understand the genomic localization of piRNAs in retina/RPE, we considered minimum 3 piRNAs originating within 20 kb distance to form a cluster. Our analysis indicated that chromosome (chr) 6 harboured four piRNA clusters followed by chr 1 with three clusters. Chr 2, 5 and 16 had two piRNA clusters in each while chr 3,11,14,17 and 18 expressed one piRNA cluster. Interestingly, 2 piRNA clusters had its origin in mitochondrial genome, which is in line with the recent identification of piR-36707 and piR-36741 in mitochondria of the mammalian cancer cells³² (Table 1).

Enriched motifs

Though piRNAs are not conserved across species, these small RNAs have been observed to possess short motifs. We identified 3 conserved motifs in piRNAs using motif predictor MEME and the first motif (21 nt long) with an E-value of 5.4×10^{-127} was conserved in 38 piRNA sequences. Further, the function and localization of the nucleotide motif was predicted using GOMo which showed that the nucleotide sequences in the first motif was found to be involved

in rRNA processing and localized to nucleolus and cytoplasm. The second motif (21 nt long) with an E-value of 1.3×10^{-23} was conserved in 14 piRNAs and was predicted to be localized in mitochondria. The third motif (28 nt long) with an E-value of 2.2×10^{-16} , speculated to reside in extracellular region, was conserved in 21 piRNA sequences. This particular motif is predicted to be involved in G-protein coupled protein receptor signalling pathway and sensory perception (Fig. 4a).

Transcription factors regulating piRNAs

Given the presence of piRNAs in human retina and RPE, we further attempted to describe the possible regulatory factors of piRNA. Sequences upstream of the piRNA loci were searched for the presence of transcription factor binding sites (Fig. 4b). It is interesting to note that transcription factor c-Rel showed higher number of binding sites in the promoters of piRNAs followed by Hepatic Leukemia factor (HLF). c-Rel is a member of NFkB transcription factor family and we also observed binding sites for NFkB in the promoters of piRNA. Though c-Rel defects are mainly associated with inflammatory disorders they are also associated with memory and synaptic plasticity³³. Meanwhile, piRNAs were also reported to be crucial for synaptic plasticity and memory storage by regulating CREB¹⁸. Our data indicated that there were binding sites for CREB in the promoter regions of the piRNAs. c-Rel, HLF, Evi-1, CCAAT-displacement protein (CDP) and Nkx2-5 were the transcription factors which contained the most number of binding sites in the analysed regions.

Evaluation of the identified piRNAs in human retina and RPE samples

Out of the 102 identified piRNAs, we evaluated the expression of piR-31068 (abundant in both retina and RPE), piR-35411 (abundant in RPE), piR-36742, piR-62011 (abundant in retina) and piR-60576 (moderate expression in both the tissues). qPCR was done in human retina and RPE tissues dissected from donor eyes which confirmed the expression of these piRNAs (Fig. 5a).

cDNA conversion without the addition of reverse transcriptase (or) the cDNA that were converted using random primers did not result in amplification indicating the specificity of the reaction. Among the piRNAs that were evaluated, piR-31068 is abundantly expressed (with low ΔCq), which is in accordance with the TPM values obtained (Table S1).

To validate whether the amplicons are indeed piRNAs, we used Reverse Transcription at Low dNTP concentration followed by PCR (RTL-P) analysis. This method investigated 2' O - methylation at the 3` ends of piRNAs. Reverse transcriptase stalls at methylated sites at low dNTP concentration. Exploiting this feature of the enzyme, piRNAs and miR-26a (control) were amplified at both high and low concentration of dNTP. During amplification, two different primers were used – unanchored³⁴ (3` methylation site of the piRNA will not be covered) and anchored (3` methylation site of the piRNA will be covered by the primer) primers. Amplification of piRNAs in the presence of unanchored primer at low dNTP concentration was low whereas it was more at high dNTP concentration. miR-26a which was not methylated at its 3` ends did not show such changes (Fig.5b). Hence, the methylation at 3` ends of the amplicons further confirmed that the obtained bands were indeed piRNAs. Altogether, our data confirmed the expression of piRNAs in human retina and RPE tissues.

Putative targets of piRNAs

We used miRanda algorithm to identify the putative targets of piRNAs, to gain insight into the possible regulatory function. We obtained a list of potential targets with a threshold score of 200 and a minimum energy value of -20 kCal/Mol (Table S3). When the targets were functionally annotated, we observed that 24% of them were uncharacterised proteins. Majority of the putative targets were channels, transporters and proteins necessary for signal transduction followed by 13% and 14% of proteins essential for metabolism and nucleotide binding respectively. Around 9% of the proteins are involved in intracellular trafficking and

7% belongs to proteins important for adhesion, cytoskeletal arrangements and cell-cell contact including tight junction proteins. The other predicted targets are known to be crucial for immune and stress response, sensory perception, neuronal activity and DNA repair (Fig. 6a).

Evaluation of the predicted targets of piRNA

Among the predicted targets, the possible influence of piRNAs in cell signalling and cell adhesion proteins can be conjectured from our previous study²¹. We demonstrated the function of HIWI2 in altering the tight junction proteins through Akt/GSK3 β signalling pathway²¹. Since PIWI proteins bind with piRNAs, effect of HIWI2 on tight junctions might be plausibly through piRNAs. Next, we analysed whether absence of piRNAs influenced the expression of putative targets. HIWI2, a ubiquitously present member of 4 PIWI-like proteins in human, was efficiently silenced in ARPE19 (RPE) cell line as indicated by the Western blot (Fig. 6b). Accordingly, the piRNAs were downregulated in Si-HIWI2 cells (Fig. 6c) and the interesting novel targets from intracellular trafficking machinery were analysed. We screened for the expression of *SNAREs* and *Rab* transcripts upon HIWI2 silencing in ARPE19 by semi RT-PCR (Fig. 6d). Further qRT-PCR indicated that *STX1A*, *Rab5*, *Rab8*, *VAMP7* and *VAMP8* were significantly downregulated in Si-HIWI2 cells (Fig. 6e). In addition, the expression of other predicted targets such as *TIMELESS*, *RPGRIP1* and *LRPAP1* were also evaluated. Strikingly, *TIMELESS* transcripts were 4.34-fold downregulated in the absence of HIWI2 (Fig. 6f). Both, *RPGRIP1* and *LRPAP1* transcripts were 3.57-fold and 1.51-fold downregulated in Si-HIWI2 cells respectively (Fig. 6f). Notably, it was reported that *RPGRIP1* mutant of Zebrafish did not develop rod outer segments in the retina and were suggested to regulate ciliary protein trafficking³⁵. *LRPAP1* is known to be associated with myopia³⁶ and the variations in *LRPAP1* were observed to be associated with late onset of Alzheimer's disease³⁷. Thus, loss of piRNAs downregulated the expression of *SNAREs*, *Rabs* and *RPGRIP1* which are important for ciliary

trafficking. In addition, *LRPAP1* and the expression of key circadian clock protein, *TIMELESS* were also reduced in the absence of piRNAs.

Elevated levels of piRNA under oxidative stress

Oxidative stress is a major cause in the pathogenesis of ocular diseases such as keratoconus, cataractogenesis and age-related macular degeneration³⁸. To gain insight into the importance of piRNAs in pathological conditions, ARPE19 cells were subjected to oxidative stress. Upon treatment of the cells with 200 μ M of H₂O₂, the piRNAs were significantly upregulated. We observed 2.3-fold upregulation of piR-36742 followed by 1.9-fold increase in piR-35411, piR-31068, piR-62011 and 1.7-fold upregulation in piR-60576 (Fig. 6g). Clearly, the expression of piRNAs were altered under oxidative stress.

Alignment of piRNA with miRNA and long non-coding RNA (lncRNA)

Since the crosstalk between the non-coding RNAs is evolving³⁹, we investigated the miRNAs and lncRNAs that might be related to the identified piRNAs. Alignment of the piRNA sequences with miRNAs showed that piR-35059, piR-36741 and piR-62011 matched with the seed sequences of miR-4420, miR-4284 and miR-182 respectively (Fig 7a). It was interesting to note that piR-62011, an abundant piRNA in retina showed complete sequence homology to miR-182, which was reported to be the highly expressed miRNA in human retina²³. Further, to understand whether the expression of piR-62011 and miR-182 are related, we examined whether silencing HIWI2 (thereby the loss of piRNAs) alters the expression of miR-182 in Y79, a retinoblastoma cell line. Remarkably, the expression of both piR-62011 and miR-182 were reduced 1.30 and 3.13- fold in HIWI2 silenced Y79 cells respectively (Fig 7b & c).

Additionally, some piRNAs showed an exact sequence match with 20 lncRNAs and few with either 1 or 2 mismatches. Many of the lncRNAs that mapped with the piRNAs were

uncharacterised (Table S4). Apparently, the sequence similarities between miR/piR/lncRNA hint a potential crosstalk among the non-coding RNAs in the retina.

Discussion

Recently, we reported the presence of PIWI-like proteins in ocular tissues and the importance of HIWI2 in the maintenance of epithelial integrity of RPE. Since PIWI proteins are associated with piRNAs, it was compelling to examine whether piRNAs play a role in retinal function. The present study confirmed the expression of piRNAs in retina and RPE. Moreover, loss of piRNAs altered the expression of specific transcripts involved in intracellular trafficking, sensory perception and circadian rhythm. We have also observed elevated levels of piRNAs under oxidative stress denoting their association with pathological conditions.

Our analysis showed that majority of the piRNAs in retina and RPE originate from tRNA fragments of Val and Gly, which is in line with the findings in human brain²⁰ and ovarian cancer tissues²⁶. Although, recent studies demonstrated the existence of small nucleolar-RNA (sno-RNA) derived piRNAs and a novel pathway for gene regulation^{30,40}, still, far less is known about this group of piRNAs. The SNORD family derived piRNAs in retina/RPE may play important functions which warrants further investigation.

It was surprising to find that piR-62011, an abundant piRNA in retina displayed seed sequence match and aligned completely with miR-182. Notably, seed sequence similarity between miR-17-5p and piRNAs has been shown to reciprocally regulate each other during mouse embryonic development⁴¹. However, the expression of miR-182 positively correlated with piR-62011. Rinck *et al* has shown that binding of multiple miRNAs with a single mRNA may either have independent or cooperative regulation among them⁴². Likewise, in a recent study piRNAs have been shown to act similar to miRNAs in targeting the mRNA with cooperative regulation⁴³. Taken together, based on the expression of piR-62011 and miR-182, they may have cooperative

activity rather than reciprocal regulation. This can be further justified by the fact that the binding sites of piR-62011 and miR-182 predicted by RNA Hybrid⁴⁴ in few selected target mRNAs, varied from very distal to very close or adjacent implying either independent or cooperative regulation between piRNAs and miRNAs. The presence of two classes of small non-coding RNAs with similar sequences points out a possibility that PIWI could bind and facilitate the miRNAs. This notion can be substantiated by the recent finding that PIWI is required for the expression of a subset of miRNAs in mouse⁴⁵.

Notably, miR-183/96/182 is reported as ‘sensory organ specific’ miRNA cluster abundantly expressed in mouse retina⁴⁶. Moreover, this cluster is modulated by light-dark adaptation⁴⁷. In support of these findings, absence of miR-182 and miR-183 lead to the loss of cone outer segments and were also described to be necessary for the formation of inner segments, connecting cilia and short outer segments of photoreceptor in adult mice². Moreover, miR-183/96/182 has been downregulated in a mouse model for inherited blindness⁴⁸. Further, miR-182 is associated with an ocular pathology called primary open-angle glaucoma⁴⁹. Hence, we speculate an independent or co-operative regulation between piR-62011 and the sensory organ specific miR-183/96/182 through seed sequence match. It would be relevant to investigate the role of piR-62011 in glaucoma and retinal degeneration.

It is interesting to note the three conserved motifs in retina and RPE. Earlier, Grivna *et al* have observed an 8-nt motif shared by 17 sequences and a 21-nt motif shared by 5 sequences, among the 40 piRNAs they have cloned from germline of male mouse⁶. Watanabe *et al* also observed 5 motifs in the germline small RNAs (gsRNA) of mouse⁵. Our bioinformatic analysis predicted, nucleus and mitochondria as the localization signal for the first motif. Accordingly, the piRNAs are reported to be observed in mitochondria of cancer cells³² and nucleus of *Aplysia* neurons¹⁸. Out of the 102 piRNAs, 7 of them mapped to the ribosomal proteins (Table S1) implicating their probable role in rRNA processing, which is in line with the functional prediction of

piRNAs. The third motif identified from our study is predicted to be involved in sensory perception which could be one of the novel functions of piRNAs in retina.

As the expression of piRNAs were reported to be tissue-specific³¹, our data also indicates that there are only 5 piRNAs in common among so far reported human tissues – brain²⁰, cardiac progenitors and cardiac fibroblasts²⁵, ovary²⁶ and testis²⁷. It is interesting to note that 75% of piRNAs in retina/RPE showed similarities with the piRNAs reported in human brain (668 piRNAs) although testis had a larger number of annotated piRNAs (11680 piRNAs) suggesting that a subset of piRNAs could be enriched in neurons. Our findings aligned with the study of Martinez *et al* which described the tissue specific expression of piRNAs with the potential of special functions in various somatic tissues³¹. Tissue enrichment analysis showed that piR-62011 is abundant in retina indicating its potential as a biomarker or a therapeutic target in retinal diseases. Although, we reported only the annotated piRNAs; identification of *de novo* piRNAs in retina and RPE should shed light on more ocular specific piRNAs. In this context, investigation of piRNAs in other non-gonadal tissues is necessary, in order to categorise the tissue specific piRNAs.

Computational annotation of piRNA target sites showed potential pleiotropic roles of piRNA in retina and RPE. It is intriguing that the majority of the identified putative targets of piRNAs are yet to be characterized for their function. The largest class of the targets is involved in signal transduction. For instance, piR-Hep1, which is conserved with piR-43771, piR-43772 and piR-60565 reduces the phosphorylation levels of Akt in hepatocellular carcinoma⁵⁰ and Rajan *et al* speculated the role of piRNAs in Akt pathway⁵¹. Evidently, our initial work showed that HIWI2 silencing increased the phosphorylation of Akt and GSK3 β . We have screened 43 kinases in Si-HIWI2 cells, involved in 4 different pathways – JAK/STAT, MAPK, Akt and AMPK. Apart from modulation of Akt pathway, we observed significant variation in the phosphorylation levels of STAT3, p53, AMPK α and HSP90²¹. In the similar line, Wang *et al*

have also shown the influence of HIWI2 in the activation of MAPK/ERK, TGF β and FGF signalling pathways⁵². It is plausible that these changes could be mediated through piRNAs, suggesting its involvement in cell signalling and cell-cell contact.

Other key group of identified piRNA targets were related to specific functions of retina and we have validated the expression of selective novel targets in the absence of piRNAs. Downregulation of *STX1A*, *Rab5*, *Rab8*, *VAMP7* and *VAMP8* indicates the likely association of piRNAs in intracellular trafficking. Rab8 is suggested to participate in ciliary trafficking of rhodopsin and in the morphogenesis of rod outer segment disk⁵³. Moreover, Rab8 and Rab11 coordinates the primary ciliogenesis mainly by regulating the vesicular trafficking⁵⁴. Primary cilia is crucial for sensory perception where defects in ciliogenesis have been observed in Bardet-Biedl syndrome (BBS) and retinal degeneration is one of the primary characteristics of BBS⁵⁵. Rabin8 directly interacts with the BBSome⁵⁶ which is stimulated by Rab11⁵⁴ underscoring the importance of trafficking proteins in sensory perception. In line with our study, piR-34393 is known to target *Rab11A* in human brain²⁰. Remarkably, mutations in *RPGRIP1*, an interacting protein of RPGR (retinitis pigmentosa GTPase regulator), is associated with diseases like leber congenital amaurosis, retinitis pigmentosa and cone-rod dystrophy. It is also known to be essential for the development of rod outer segments by regulating the ciliary protein trafficking and Rab8 was observed to be mislocalized in *rpgrip1* mutants³⁵. Our data shows significant downregulation of both *Rab8* and *RPGRIP1* transcripts in the absence of piRNAs. Interestingly, expression of *RPGRIP1* was readily detected only in retina and testis when a panel of RNA from human tissues were screened⁵⁷. piRNAs, which were thought to be specific to testis, might regulate *RPGRIP1* and thus may effect neurodegeneration which needs to be confirmed by further functional experiments.

LRPAP1 (LDL receptor related protein associated protein 1), another predicted piRNA target, is also downregulated in Si-HIWI2 cells. *LRPAP1* is known to be associated with high myopia

by influencing the activity of TGF β and thereby remodelling the sclera⁵⁸. Alterations in *LRPAP1* is also related with late-onset of AD³⁷. Esposito *et al* have shown the expression of piRNAs in AD⁵⁹ and a further study demonstrated dysregulation of piRNAs in AD²⁰. Together with *RPGRIP1*, downregulation of *LRPAP1* indicates a possible role of piRNAs in retinal degeneration.

Our data also showed that TIMELESS, a protein needed for the regulation of circadian rhythm in mammals, is observed to be affected in the absence of piRNAs. Activation of circadian piRNA expression is suggested to be a strategy adopted by *Drosophila melanogaster* to maintain the genomic integrity during aging⁶⁰. Furthermore, the role of PIWIL2 in suppressing the degradation of circadian proteins CLOCK and BMAL1 through phosphorylation of Akt/GSK3 β and by binding to the E-box sequences of BMAL1/CLOCK complex, confirms the importance of PIWI-like proteins in regulating circadian rhythms⁶¹. It is worth noting that miR-182 is known to target the 3'UTR of *CLOCK* mRNA^{62,63} and is inhibited by GSK3 β ⁶⁴. Similarly, HIWI2 also affects the Akt/GSK3 β pathway²¹ and as mentioned earlier, piR-62011 aligns exactly with the seed sequence of miR-182 indicating a potential functional interaction between piR-62011/miR-182 in influencing the activity of CLOCK-controlled genes. In addition, improper processing of pre-miR-182 is documented to be the major cause of depression in insomnia patients⁶³. Hence, it would be interesting to explore the regulatory role played by piRNAs and miRNAs in the circadian rhythm related disorders.

It is intriguing that the examined targets were all downregulated at transcript level although they were selected based on complementarity using miRanda. It is known that piRNAs regulate the expression of genes by imperfect base-pairing rule⁶⁵, a mechanism similar to miRNAs. The possible mechanism behind the repression of the transcripts could be epigenetic activation⁶⁶ or silencing¹⁸ through repressive epigenetic marks by piRNAs at the transcriptional level.

Nevertheless, we cannot rule out the mechanism of posttranscriptional regulation by piRNAs as shown in transposon-driven mRNAs⁶⁷.

Our data showed that expression of piRNAs are elevated under oxidative stress. Martinez *et al* recently reported 40 piRNAs that were regulated by hypoxia in tumors⁶⁸. It is possible that these piRNAs might have been influenced by the oxidative stress/reactive oxygen species generated by the hypoxic conditions. In eye, oxidative stress plays a major role in the pathogenesis of many diseases such as keratoconus, Fuchs' endothelial corneal dystrophy, Leber's hereditary optic neuropathy and cataractogenesis³⁸. ROS and oxidative stress is also known to stimulate inflammation and pathological angiogenesis in diabetic retinopathy and it plays a pivotal role in the pathogenesis of age-related macular degeneration³⁸. Thus, several evidences indicate a potential role of piRNAs in retinal pathologies.

Conclusion

Our study showed the first line of evidence for the presence of piRNAs in human retina and RPE. We have further identified and validated novel targets of piRNAs which are essential for fundamental functions of retina and RPE. The intriguing finding of our analysis is the seed sequence similarity between piR62011 and sensory organ specific miR183/96/182 cluster. The crosstalk may modulate the unique cellular demands of retina, such as, circadian expression of phototransduction components and polarized trafficking in photoreceptors. Our study also hints the possibility of interplay between piRNAs and miRNAs in regulating gene expression at transcriptional or post transcriptional level. In addition, altered expression of piRNAs under oxidative stress implies their role in pathological conditions. In summary, our finding highlights the significance of PIWI/piRNAs in visual function and retinal degeneration.

Materials and methods

Data source

Small RNA sequencing datasets of human retina and RPE was downloaded from (Accession ID: E-MTAB-3792)²³. The dataset consisted of 16 human retina and 2 RPE tissue samples. The datasets ERR973601-ERR973608 and ERR973611-ERR673618 were retinal samples. ERR973609 and ERR973610 were RPE datasets.

Data processing

Adapter sequences present in the datasets were removed using Cutadapt⁶⁹ with PHRED score 30 and the sequences less than 20 nt were filtered out. The reads which mapped to other non-coding RNAs (tRNA, snRNA, snoRNA, miRNA, rRNA, mtRNA) were discarded and the unmapped reads were taken for further analysis. miRNA sequences were downloaded from miRBase^{70,71} and all other RNA sequences were retrieved from Pfam⁷². The reads were mapped using BOWTIE⁷³.

Identification and differential expression of known piRNAs

After eliminating the known annotated small RNAs, unique reads and read count from the data were retrieved using `unique_reads_for_mapping.pl` from miRGrep tool⁷⁴. Unique reads were aligned to the known piRNA database downloaded from piRNAquest²⁴ using `soap.short` tool⁷⁴ with default parameters (allowed 2bp mismatches). Output file was used to calculate the final read count using 'awk' command and retain the piRNAs which are having ≥ 10 read count in any one library. Details of the origin of piRNAs were retrieved from piRNAQuest²⁴ and the piRNAs were categorised as clusters when minimum of 3 piRNAs originated within 20 Kbp.

The quantification of each piRNA in each library was normalized to TPM (Tags per million reads) and further converted to Log2 values. Before Log2 conversion, piRNAs which were

having zero TPM in any one of the library were removed. Log₂ values were used in Morpheus to generate heatmap.

Tissue enrichment analysis

piRNAs annotated in brain²⁰, cardiac progenitors and fibroblasts²⁵, ovary²⁶ and testis²⁷ were downloaded. In case of human brain, piRNAs reported in both healthy and AD brain were combined and the duplicates were removed which amounted to 668 in total. For piRNAs in cardiac progenitors and cardiac fibroblasts, the piRNAs listed in cardiospheres, cardiosphere-derived cells and cardiac fibroblasts were combined and the redundant entries were eliminated resulting to 2366 piRNAs. Out of 20121 piRNAs in human testis, same piRNAs of varying lengths were considered as one entry and a total of 11680 piRNAs were compared with retina/RPE. InteractiVenn⁷⁵ was used for tissue enrichment analysis.

Motif prediction and lncRNA/miRNA/piRNA alignment

Motifs in the piRNA sequences were predicted using MEME software⁷⁶ with site distribution parameter to be any number of repetitions and the putative functions of the motifs were analysed by GOMo⁷⁶ with the default factors. Soap.short tool⁷⁴ was used to compare the identified piRNA sequences with the lncRNA sequences downloaded from the database LNCipedia^{77,78}. The alignment was performed with the default parameters allowing maximum number of 2 bp mismatches. Human miRNA sequences from miRbase were aligned with the identified piRNAs to analyse seed sequence similarity and the alignments with the maximum of 2 mismatches are listed in Supplementary table S3.

Identification of transcription factor binding sites

We analysed the Transcription start site (TSS), promoter and TFBS for the piRNA genes. Human promoter prediction tool, FPROM⁷⁹ was used to predict the TSS and promoter site within the 10 kb upstream of the piRNA locus, extracted from the UCSC table browser. TFBS

was scanned 1kb upstream of each piRNA using P-Match 1.0⁸⁰ with vertebrate matrix groups and the cut-off has chosen to minimize the sum of both false positive and false negative error rates.

Prediction of piRNA targets

Targets of piRNAs were predicted using miRanda v3.3a algorithm⁸¹⁻⁸³ with the following parameters: Gap Open Penalty (-9.0); Gap Extend Penalty (-4.0); Score Threshold (200.0); Energy Threshold (1.0 kcal/mol); Scaling Parameter (4.0). The hits which had score ≥ 200 and energy value ≤ -20 kcal/Mol were considered to be the putative targets.

Ethics statement

Donor eyes were obtained from CU Shah eye bank, Sankara Nethralaya with prior approval from the Institutional Review Board and Ethics Sub-Committee of Vision Research Foundation, Chennai, India. Eye globes were collected from donors after obtaining informed consent from their family. The experiments involving usage of the ocular tissues were carried out according to the Tenets of the Declaration of Helsinki.

Cell culture

ARPE19 cells (ATCC-CRL-2302) (ATCC, USA) and Y79 cells were cultured using DMEM-F12 (Sigma Aldrich, USA) and RPMI-1640 respectively with 10% (v/v) heat-inactivated Fetal Bovine Serum (ThermoFisher Scientific, USA) and was maintained at 37°C in 5% CO₂ incubator. ARPE19 cells were passaged the day before transfection whereas Y79 cells were passaged on the same day of transfection and 2 X 10⁵ cells were seeded in a 6-well plate. DsiRNA specific to 3' UTR of HIWI2 (Integrated DNA Technologies, USA) was transfected using Lipofectamine RNAiMAX (ThermoFisher Scientific, USA) according to manufacturer's instruction. Scrambled sequence was used as experimental control and RNA was isolated from Si-Control and Si-HIWI2 cells, 48 h post transfection. To induce oxidative stress, the cells were

treated with 200 μ M H₂O₂ for 24 h and RNA was isolated from the same to check for the expression of piRNAs.

Real time PCR

Primers for piRNA and miRNA amplification were designed using miR2 primer software⁸⁴. cDNA conversion was done with 1 μ g of RNA based on the protocol by Busk and Cirera, 2014⁸⁵. The cocktail for cDNA conversion contained Poly A polymerase (New England Biolabs, USA) for adding poly A tail; M-MuLV reverse transcriptase (New England Biolabs, USA) and a RT-primer of sequence - 5'-CAGGTCCAGTTTTTTTTTTTTTTTTTGC-3', to convert the poly A tailed RNA to cDNA. 25 ng of cDNA was used for amplification of piRNAs listed in Table 2. Transcripts other than small RNAs were amplified from cDNA converted using iScript cDNA synthesis kit (Biorad, USA).

Reverse Transcription at Low dNTP concentration followed by PCR (RTL-P) analysis

RTL-P analysis was carried out as described by Dong et al, 2012³⁴. RNA was converted to cDNA with low concentration of dNTP (0.4 μ M) in the presence of either unanchored primer (UAP) or anchored primer (AP). The same was done at high concentration of dNTP (40 μ M) as well. Four different cDNA ((1) Low dNTP with UAP; (2) Low dNTP with AP; (3) High dNTP with UAP; and (4) High dNTP with AP) were used to amplify piRNA and miRNA and the amplicons were run in 2% agarose gel. Primers used in the study are listed in Table 2.

Western blot

After transfection, the cells were lysed using Radio Immunoprecipitation Assay (RIPA) buffer (150 mM NaCl, 0.1 % TritonX-100, 0.5 % sodium deoxycholate, 0.1% SDS, 50 mM Tris, pH 8.0) with protease inhibitors (1 mmol/L dithiothreitol, 0.5 mmol/L phenylmethylsulfonyl fluoride, 1 mg/mL leupeptin, 10 mmol/L p-nitrophenylphosphate, 10mmol/L h-glycerol phosphate) and were sonicated. The lysates were then centrifuged at 10, 000 rpm for 5 min and

the proteins in the supernatant were estimated by BCA protein assay reagent (Thermo Scientific, Waltham, USA). 35 µg of protein was resolved using SDS-PAGE gel and was electrotransferred to nitrocellulose membrane (GE healthcare, UK). The blots were then incubated with 5 % blocking solution for 1 h (5 % skimmed milk powder in Tris Buffered Saline) after which they were probed for either HIWI2 (Thermo Scientific, Waltham, USA) or βACTIN (Santa Cruz Biotechnology, Dallas, USA) by incubating overnight at 4°C with 1 in 1,000 dilution of primary antibody. Imaging of the blots were done using FluorChem C3 (Protein Simple, San Jose, USA) after incubating with the respective secondary antibodies (1 in 10,000 dilution) for 2 h.

Data availability

The datasets analysed were downloaded from the ArrayExpress (Accession No: E-MTAB-3792) (<https://www.ebi.ac.uk/arrayexpress/experiments/E-MTAB-3792/>).

References

1. Graw, J. Eye development. *Curr Top Dev Biol* **90**, 343–386 (2010).
2. Busskamp, V. *et al.* miRNAs 182 and 183 Are Necessary to Maintain Adult Cone Photoreceptor Outer Segments and Visual Function. *Neuron* **83**, 586–600 (2014).
3. Zelinger, L. & Swaroop, A. RNA Biology in Retinal Development and Disease. *Trends Genet* (2018). doi:10.1016/j.tig.2018.01.002
4. Aravin, A. *et al.* A novel class of small RNAs bind to MILI protein in mouse testes. *Nature* **442**, 203–7 (2006).
5. Watanabe, T. *et al.* Identification and characterization of two novel classes of small RNAs in the mouse germline: retrotransposon-derived siRNAs in oocytes and germline small RNAs in testes. *Genes Dev* **20**, 1732–1743 (2006).
6. Grivna, S. T., Beyret, E., Wang, Z. & Lin, H. A novel class of small RNAs in mouse spermatogenic cells. *Genes Dev* **20**, 1709–14 (2006).
7. Ohara, T. *et al.* The 3' termini of mouse Piwi-interacting RNAs are 2'-O-methylated. *Nat Struct Mol Biol* **14**, 349–350 (2007).
8. Kirino, Y. & Mourelatos, Z. Mouse Piwi-interacting RNAs are 2'-O-methylated at their 3' termini. *Nat Struct Mol Biol* **14**, 347–348 (2007).
9. Brennecke, J. *et al.* Discrete small RNA-generating loci as master regulators of transposon activity in *Drosophila*. *Cell* **128**, 1089–103 (2007).

10. Rizzo, F. *et al.* Timed regulation of P-element-induced wimpy testis-interacting RNA expression during rat liver regeneration. *Hepatology* **60**, 798–806 (2014).
11. Henaoui, I. S. *et al.* PIWI-interacting RNAs as novel regulators of pancreatic beta cell function. *Diabetologia* **60**, 1977–1986 (2017).
12. Yin, J. *et al.* piR-823 contributes to colorectal tumorigenesis by enhancing the transcriptional activity of HSF1. *Cancer Sci* **108**, 1746–1756 (2017).
13. Li, D. *et al.* piR-651 promotes tumor formation in non-small cell lung carcinoma through the upregulation of cyclin D1 and CDK4. *Int J Mol Med* **38**, 927–36 (2016).
14. Peng, L. *et al.* piR-55490 inhibits the growth of lung carcinoma by suppressing mTOR signaling. *Tumour Biol* **37**, 2749–56 (2016).
15. Rajan, K. S. *et al.* Abundant and Altered Expression of PIWI-Interacting RNAs during Cardiac Hypertrophy. *Hear Lung Circ* **25**, 1013–1020 (2016).
16. Lee, E. J. *et al.* Identification of piRNAs in the central nervous system. *RNA* **17**, 1090–1099 (2011).
17. Dharap, A., Nakka, V. P. & Vemuganti, R. Altered Expression of PIWI RNA in the Rat Brain After Transient Focal Ischemia. *Stroke* **42**, 1105–1109 (2011).
18. Rajasethupathy, P. *et al.* A Role for Neuronal piRNAs in the Epigenetic Control of Memory-Related Synaptic Plasticity. *Cell* **149**, 693–707 (2012).
19. Phay, M., Kim, H. H. & Yoo, S. Analysis of piRNA-Like Small Non-coding RNAs Present in Axons of Adult Sensory Neurons. *Mol Neurobiol* **55**, 483–494 (2018).
20. Roy, J., Sarkar, A., Parida, S., Ghosh, Z. & Mallick, B. Small RNA sequencing revealed dysregulated piRNAs in Alzheimer’s disease and their probable role in pathogenesis. *Mol Biosyst* **13**, 565–576 (2017).
21. Sivagurunathan, S., Palanisamy, K., Arunachalam, J. P. & Chidambaram, S. Possible role of HIWI2 in modulating tight junction proteins in retinal pigment epithelial cells through Akt signaling pathway. *Mol Cell Biochem* **427**, 145–156 (2017).
22. Sivagurunathan, S., Arunachalam, J. P. & Chidambaram, S. PIWI-like protein, HIWI2 is aberrantly expressed in retinoblastoma cells and affects cell-cycle potentially through OTX2. *Cell Mol Biol Lett* **22**, 17 (2017).
23. Karali, M. *et al.* High-resolution analysis of the human retina miRNome reveals isomiR variations and novel microRNAs. *Nucleic Acids Res* **44**, 1525–40 (2016).
24. Sarkar, A., Maji, R. K., Saha, S. & Ghosh, Z. piRNAQuest: searching the piRNAome for silencers. *BMC Genomics* **15**, 555 (2014).
25. Vella, S. *et al.* PIWI-interacting RNA (piRNA) signatures in human cardiac progenitor cells. *Int J Biochem Cell Biol* **76**, 1–11 (2016).
26. Singh, G., Roy, J., Rout, P. & Mallick, B. Genome-wide profiling of the PIWI-interacting RNA-mRNA regulatory networks in epithelial ovarian cancers. *PLoS One* **13**, e0190485 (2018).
27. Yang, Q. *et al.* MicroRNA and piRNA Profiles in Normal Human Testis Detected by Next Generation Sequencing. *PLoS One* **8**, e66809 (2013).

28. Keam, S. P. *et al.* The human Piwi protein Hiwi2 associates with tRNA-derived piRNAs in somatic cells. *Nucleic Acids Res* **42**, 8984–95 (2014).
29. Robine, N. *et al.* A Broadly Conserved Pathway Generates 3'UTR-Directed Primary piRNAs. *Curr Biol* **19**, 2066–2076 (2009).
30. Zhong, F. *et al.* A SnoRNA-derived piRNA interacts with human interleukin-4 pre-mRNA and induces its decay in nuclear exosomes. *Nucleic Acids Res* **43**, gkv954 (2015).
31. Martinez, V. D. *et al.* Unique somatic and malignant expression patterns implicate PIWI-interacting RNAs in cancer-type specific biology. *Sci Rep* **5**, 10423 (2015).
32. Kwon, C. *et al.* Detection of PIWI and piRNAs in the mitochondria of mammalian cancer cells. *Biochem Biophys Res Commun* **446**, 218–223 (2014).
33. Gilmore, T. D. & Gerondakis, S. The c-Rel Transcription Factor in Development and Disease. *Genes Cancer* **2**, 695–711 (2011).
34. Dong, Z.-W. *et al.* RTL-P: a sensitive approach for detecting sites of 2'-O-methylation in RNA molecules. *Nucleic Acids Res* **40**, e157 (2012).
35. Raghupathy, R. K. *et al.* Rpgr1p1 is required for rod outer segment development and ciliary protein trafficking in zebrafish. *Sci Rep* **7**, 16881 (2017).
36. Khan, A. O., Aldahmesh, M. A. & Alkuraya, F. S. Clinical Characterization of LRPAP1-Related Pediatric High Myopia. *Ophthalmology* **123**, 434–435 (2016).
37. Sánchez, L. *et al.* Variation in the LRP-associated protein gene (LRPAP1) is associated with late-onset Alzheimer disease. *Am J Med Genet* **105**, 76–8 (2001).
38. Nita, M. & Grzybowski, A. The Role of the Reactive Oxygen Species and Oxidative Stress in the Pathomechanism of the Age-Related Ocular Diseases and Other Pathologies of the Anterior and Posterior Eye Segments in Adults. *Oxid Med Cell Longev* **2016**, 3164734 (2016).
39. Yamamura, S., Imai-Sumida, M., Tanaka, Y. & Dahiya, R. Interaction and cross-talk between non-coding RNAs. *Cell Mol Life Sci* **75**, 467–484 (2018).
40. He, X. *et al.* An Lnc RNA (GAS5)/SnoRNA-derived piRNA induces activation of TRAIL gene by site-specifically recruiting MLL/COMPASS-like complexes. *Nucleic Acids Res* **43**, 3712–25 (2015).
41. Du, W. W. *et al.* Reciprocal regulation of miRNAs and piRNAs in embryonic development. *Cell Death Differ* **23**, 1458–1470 (2016).
42. Rinck, A. *et al.* The human transcriptome is enriched for miRNA-binding sites located in cooperativity-permitting distance. *RNA Biol* **10**, 1125–1135 (2013).
43. Shen, E.-Z. *et al.* Identification of piRNA Binding Sites Reveals the Argonaute Regulatory Landscape of the *C. elegans* Germline. *Cell* **172**, 937–951.e18 (2018).
44. Rehmsmeier, M., Steffen, P., Hochsmann, M. & Giegerich, R. Fast and effective prediction of microRNA/target duplexes. *RNA* **10**, 1507–17 (2004).
45. Grivna, S. T., Pyhtila, B. & Lin, H. MIWI associates with translational machinery and PIWI-interacting RNAs (piRNAs) in regulating spermatogenesis. *Proc Natl Acad Sci*

- 103**, 13415–13420 (2006).
46. Xu, S., Witmer, P. D., Lumayag, S., Kovacs, B. & Valle, D. MicroRNA (miRNA) Transcriptome of Mouse Retina and Identification of a Sensory Organ-specific miRNA Cluster. *J Biol Chem* **282**, 25053–25066 (2007).
 47. Krol, J. *et al.* Characterizing Light-Regulated Retinal MicroRNAs Reveals Rapid Turnover as a Common Property of Neuronal MicroRNAs. *Cell* **141**, 618–631 (2010).
 48. Palfi, A. *et al.* microRNA regulatory circuits in a mouse model of inherited retinal degeneration. *Sci Rep* **6**, 31431 (2016).
 49. Liu, Y. *et al.* A Common Variant in *MIR182* Is Associated With Primary Open-Angle Glaucoma in the NEIGHBORHOOD Consortium. *Investig Ophthalmology Vis Sci* **57**, 4528 (2016).
 50. Law, P. T.-Y. *et al.* Deep sequencing of small RNA transcriptome reveals novel non-coding RNAs in hepatocellular carcinoma. *J Hepatol* **58**, 1165–73 (2013).
 51. Rajan, K. S., Velmurugan, G., Pandi, G. & Ramasamy, S. miRNA and piRNA mediated Akt pathway in heart: antisense expands to survive. *Int J Biochem Cell Biol* **55**, 153–6 (2014).
 52. Wang, Z., Liu, N., Shi, S., Liu, S. & Lin, H. The Role of PIWIL4, an Argonaute Family Protein, in Breast Cancer. *J Biol Chem* **291**, 10646–58 (2016).
 53. Deretic, D. *et al.* rab8 in retinal photoreceptors may participate in rhodopsin transport and in rod outer segment disk morphogenesis. *J Cell Sci* **108** (Pt 1), 215–24 (1995).
 54. Knödler, A. *et al.* Coordination of Rab8 and Rab11 in primary ciliogenesis. *Proc Natl Acad Sci U S A* **107**, 6346–51 (2010).
 55. Marshall, W. F. The cell biological basis of ciliary disease. *J Cell Biol* **180**, 17–21 (2008).
 56. Nachury, M. V *et al.* A core complex of BBS proteins cooperates with the GTPase Rab8 to promote ciliary membrane biogenesis. *Cell* **129**, 1201–13 (2007).
 57. Boylan, J. P. & Wright, A. F. Identification of a novel protein interacting with RPGR. *Hum Mol Genet* **9**, 2085–93 (2000).
 58. Aldahmesh, M. A. *et al.* Mutations in LRPAP1 are associated with severe myopia in humans. *Am J Hum Genet* **93**, 313–20 (2013).
 59. Esposito, T., Magliocca, S., Formicola, D. & Gianfrancesco, F. piR_015520 belongs to Piwi-associated RNAs regulates expression of the human melatonin receptor 1A gene. *PLoS One* **6**, e22727 (2011).
 60. Kuintzle, R. C. *et al.* Circadian deep sequencing reveals stress-response genes that adopt robust rhythmic expression during aging. *Nat Commun* **8**, 14529 (2017).
 61. Lu, Y. *et al.* Cancer/testis antigen PIWIL2 suppresses circadian rhythms by regulating the stability and activity of BMAL1 and CLOCK. *Oncotarget* **8**, 54913–54924 (2017).
 62. Ding, X. *et al.* The role of miR-182 in regulating pineal CLOCK expression after hypoxia-ischemia brain injury in neonatal rats. *Neurosci Lett* **591**, 75–80 (2015).
 63. Saus, E. *et al.* Genetic variants and abnormal processing of pre-miR-182, a circadian

- clock modulator, in major depression patients with late insomnia. *Hum Mol Genet* **19**, 4017–4025 (2010).
64. Tang, X. *et al.* Glycogen synthase kinase 3 beta inhibits microRNA-183-96-182 cluster via the β -Catenin/TCF/LEF-1 pathway in gastric cancer cells. *Nucleic Acids Res* **42**, 2988–98 (2014).
 65. Gou, L.-T. *et al.* Pachytene piRNAs instruct massive mRNA elimination during late spermiogenesis. *Cell Res* **24**, 680–700 (2014).
 66. Yin, H. & Lin, H. An epigenetic activation role of Piwi and a Piwi-associated piRNA in *Drosophila melanogaster*. *Nature* **450**, 304–308 (2007).
 67. Watanabe, T. & Lin, H. Posttranscriptional Regulation of Gene Expression by Piwi Proteins and piRNAs. *Mol Cell* **56**, 18–27 (2014).
 68. Martinez, V. D. *et al.* Non-coding RNAs predict recurrence-free survival of patients with hypoxic tumours. *Sci Rep* **8**, 152 (2018).
 69. Martin, M. Cutadapt removes adapter sequences from high-throughput sequencing reads. *EMBnet.journal* **17**, (2011).
 70. Griffiths-Jones, S. The microRNA Registry. *Nucleic Acids Res* **32**, 109D–111 (2004).
 71. Griffiths-Jones, S., Grocock, R. J., van Dongen, S., Bateman, A. & Enright, A. J. miRBase: microRNA sequences, targets and gene nomenclature. *Nucleic Acids Res* **34**, D140–4 (2006).
 72. Finn, R. D. *et al.* The Pfam protein families database: towards a more sustainable future. *Nucleic Acids Res* **44**, D279–85 (2016).
 73. Langmead, B., Trapnell, C., Pop, M. & Salzberg, S. L. Ultrafast and memory-efficient alignment of short DNA sequences to the human genome. *Genome Biol* **10**, R25 (2009).
 74. Li, N. *et al.* Global profiling of miRNAs and the hairpin precursors: insights into miRNA processing and novel miRNA discovery. *Nucleic Acids Res* **41**, 3619–34 (2013).
 75. Heberle, H., Meirelles, G. V., da Silva, F. R., Telles, G. P. & Minghim, R. InteractiVenn: a web-based tool for the analysis of sets through Venn diagrams. *BMC Bioinformatics* **16**, 169 (2015).
 76. Bailey, T. L. *et al.* MEME SUITE: tools for motif discovery and searching. *Nucleic Acids Res* **37**, W202–8 (2009).
 77. Volders, P.-J. *et al.* LNCipedia: a database for annotated human lncRNA transcript sequences and structures. *Nucleic Acids Res* **41**, D246–51 (2013).
 78. Volders, P.-J. *et al.* An update on LNCipedia: a database for annotated human lncRNA sequences. *Nucleic Acids Res* **43**, D174–D180 (2015).
 79. Solovyev, V., Kosarev, P., Seledsov, I. & Vorobyev, D. Automatic annotation of eukaryotic genes, pseudogenes and promoters. *Genome Biol* **7 Suppl 1**, S10.1–12 (2006).
 80. Chekmenev, D. S., Haid, C. & Kel, A. E. P-Match: transcription factor binding site

- search by combining patterns and weight matrices. *Nucleic Acids Res* **33**, W432-7 (2005).
81. Enright, A. J. *et al.* MicroRNA targets in Drosophila. *Genome Biol* **5**, R1 (2003).
 82. Betel, D., Wilson, M., Gabow, A., Marks, D. S. & Sander, C. The microRNA.org resource: targets and expression. *Nucleic Acids Res* **36**, D149-53 (2008).
 83. John, B. *et al.* Human MicroRNA Targets. *PLoS Biol* **2**, e363 (2004).
 84. Busk, P. K. A tool for design of primers for microRNA-specific quantitative RT-qPCR. *BMC Bioinformatics* **15**, 29 (2014).
 85. Cirera, S. & Busk, P. K. in *Methods in molecular biology (Clifton, N.J.)* **1182**, 73–81 (2014).

Acknowledgements

We acknowledge the financial assistance provided by Department of Science and Technology under the project “SR/FT/LS-145/2010” and Department of Biotechnology under the project DBT-Neurobiology Taskforce - “BT/PR5055/MED/30/761/2012”. The funding body is not involved in the design of the study and collection, analysis, and interpretation of data and in writing the manuscript. We thank Indian Council of Medical Research project “BMS/FW/BIOCHEM/2015-23270/OCT-2015/24/TN/PVT” and Max Planck-India mobility grant ‘IGSTC/MPG/FS (SC)2012’. CS thanks the support from University Grants Commission, New Delhi for the award of Assistant Professorship under its Faculty Recharge Program (UGC-FRP) and for the start-up grant.

Author contributions

SS designed, performed the *in vitro* experiments; part of *in silico* experiments and wrote the manuscript. SN performed *in silico* experiments. PG and AJ interpreted the data and reviewed the manuscript. CS conceived the idea, received the funding, planned the experiments and reviewed the manuscript. All authors read and approved the final manuscript.

Competing interests

The authors declare no competing interests.

Figure legends

Fig 1. Workflow of piRNA identification. The flowchart describes the step by step protocol of piRNA analysis using the small RNA sequencing dataset of human retina and retinal pigment epithelium.

Fig 2. In silico analysis for identification of piRNAs in human retina and retinal pigment epithelium (RPE). a) Heatmap shows the expression of the identified 102 piRNAs in human retina (16 datasets) and RPE (2 dataset). b) Heatmap depicts the differential expression of piRNAs in retina and RPE. Tags per million (TPM) values are used to generate heatmap using Morpheus. c) Venn diagram depicts the unique and commonly expressed piRNAs in 6 human tissues, retina and RPE; brain; cardiac progenitors and cardiac fibroblasts; ovary and testis.

Fig 3. Genomic origin of piRNAs. a) Bar graph depicts the data obtained from piRNAQuest with the number of piRNAs that originate from the mentioned genomic regions. b) A representative list of identified piRNAs with piRNABank ID, sequence and genomic origin are presented in the table. This list also includes the 5 piRNAs validated in the study.

Fig 4. Enriched motifs and regulators of piRNAs. a) Logos with the corresponding E-values represent the motifs identified by MEME. Function and cellular localization of the motifs predicted by GOMo are also shown. b) Bar graph represents the number of transcription factor binding sites observed in the upstream sequences of 102 piRNAs.

Fig 5. Validation of piRNA expression in human retina and RPE tissues. a) Bar graph represents the average ΔCq values of piRNAs (*piR-31068*, *piR-35411*, *piR-36742*, *piR-60576* and *piR-62011*) obtained using qRT-PCR from retina and RPE tissues. Since the bar graph

shows the average ΔCq values, the smaller bar represents higher expression and vice versa. The Cq values were normalized with U6. b) RTL-P analysis confirms the 3'-terminal 2'-O-methylation of piRNAs. Amplification of piRNA with unanchored primer at low dNTP concentration was reduced whereas the miRNA did not show any significant difference between unanchored and anchored primers. Full length images of the gels are presented in supplementary figure S1. (RTL-P – Reverse Transcription at Low dNTP concentration followed by PCR; UAP – Unanchored primer; AP – Anchored primer)

Fig 6. Potential targets of piRNAs. a) Pie chart shows the percentage of putative targets of piRNA in each category predicted by miRanda algorithm. b) Downregulation of HIWI2 is shown by Western blot in Si-Control and Si-HIWI2 ARPE19 cells. β ACTIN is used as loading control. Full length images of the blots are presented in supplementary figure S2. c) Expression of piRNAs in Si-HIWI2 ARPE19 cells is shown as fold change obtained by qRT-PCR. U6 levels are used for normalization. d) Agarose gel image showing the expression of *SNAREs* and *Rabs* in Si-Control and Si-HIWI2 cells. *GAPDH* is used as the loading control. e) Bar graph represents the fold change of *STX1A*, *STX6*, *STX16*, *Rab5*, *Rab8*, *VAMP7* and *VAMP8* in Si-HIWI2 ARPE19 cells obtained by qRT-PCR. *18S rRNA* is used for normalization. f) Bar graph shows the fold change of *LRPAP1*, *RPGRIP1* and *TIMELESS* in Si-HIWI2 ARPE19 cells. The expression is normalized with *18S rRNA*. g) Fold change of piRNAs obtained by qRT-PCR from the cells subjected to oxidative stress using 200 μ M H_2O_2 are depicted as bar graph. U6 is used for normalization. (* $p < 0.05$; ** $p < 0.01$; *** $p < 0.001$; Student's *t* test was used to analyse the statistical significance between Si-Control and Si-HIWI2; control and H_2O_2 treated cells)

Fig 7. miR-182 is downregulated in Si-HIWI2 Y79 cells. a) The table lists the miRNAs which showed seed sequence similarity with piRNAs. b) Western blot shows the expression of HIWI2 in Si-Control and Si-HIWI2 Y79 cells. β ACTIN is used as loading control. Full length

images of the blots are presented in supplementary figure S2. c) Bar graph represents the fold change of *piR-62011* and *miR-182* obtained by qRT-PCR in Si-Control and Si-HIWI2 Y79 cells. U6 is used for normalization. (* $p < 0.05$; Student's *t* test was used to analyse the statistical significance between Si-Control and Si-HIWI2)

Fig 8. Hypothetical model for pleiotropic functions of piRNAs. The model depicts the multiple functions of piRNAs in RPE in (1) Altering the expression of tight junctions; (2) Regulation of ciliary trafficking and sensory perception by influencing *RPGRIP1*; (3) Intracellular trafficking by affecting the expression of *STX1A*, *Rab5*, *Rab8*, *VAMP7* and *VAMP8*; (4) Regulation of circadian clock by acting on *TIMELESS*; (5) Involvement in retinal degeneration through modulation of *LRPAP1* and *RPGRIP1*. Regulation of these processes by piRNAs may include a functional interaction with miRNAs. Gaining deeper understanding of the exact molecular mechanism will expand our knowledge on pleiotropic effects of piRNAs in somatic cells. (SE: Sorting Endosome; FR: Fast Recycling; SR: Slow Recycling; LE: Late Endosome)

Table 1. Chromosomal distribution of piRNAs.

Chromosome	Number of piRNA clusters	Number of piRNAs in each cluster
Chromosome 1	3	Cluster 1 – 6 piRNAs Cluster 2 – 4 piRNAs Cluster 3 – 5 piRNAs
Chromosome 2	2	Cluster 1 – 5 piRNAs Cluster 2 – 4 piRNAs
Chromosome 3	1	Cluster 1 – 3 piRNAs
Chromosome 5	2	Cluster 1 – 5 piRNAs Cluster 2 – 9 piRNAs
Chromosome 6	4	Cluster 1 – 7 piRNAs Cluster 2 – 7 piRNAs Cluster 3 – 5 piRNAs Cluster 4 – 4 piRNAs
Chromosome 11	1	Cluster 1 – 4 piRNAs
Chromosome 14	1	Cluster 1 – 3 piRNAs
Chromosome 16	2	Cluster 1 – 6 piRNAs Cluster 2 – 4 piRNAs
Chromosome 17	1	Cluster 1 – 5 piRNAs
Chromosome 18	1	Cluster 1 – 3 piRNAs
Mitochondrial genome	2	Cluster 1 – 6 piRNAs Cluster 2- 4 piRNAs
Chromosome 4, 7, 8, 9, 10, 12, 13, 15, 19,20, 21, 22, X and Y chromosome	No clusters.	0-4 piRNAs

Table 2. Primer sequences used for RT and qRT-PCR

Name	Forward primer (5'- 3')	Reverse primer (5'- 3')
<i>piR-31068</i>	cattggtggttcagtgtag	ccagttttttttttttgcgaga
<i>piR-35411</i>	gctcagtcggtagagca	ggtccagtttttttttttctca
<i>piR-36742</i>	ttccgtagttagtggtca	tccagttttttttttttgcga
<i>piR-60576</i>	ccgtagttagtggttatcac	cagttttttttttttggcgaa
<i>piR-62011</i>	gtttgcaatggtagaactca	gtccagtttttttttttacctca
<i>miR-26a</i>	gcagttcaagtaatccaggatag	ggtccagtttttttttttagc
<i>miR-182</i>	gtttggcaatggtagaactca	ggtccagtttttttttttagtgt
<i>5.8S rRNA</i>	tcgtgcgctgatgaagaa	gaagtgtc gatgatcaatgtgtc
<i>U6</i>	gcttcggcagcacatatactaaat	cgcttcacgaatttgcgtgcat
<i>LRPAP1</i>	ggcgaagacctctgggaat	gtctccagcaggacgttgta
<i>RPGRIP1</i>	cacagcccctccatcgttta	tgatgtggcactgtaggc
<i>TIMELESS</i>	atgagacacgagatgtgcgg	gtgaggatgggcagaaggtc
<i>STX1A</i>	gaccgctcatggatgagtt	cttggaacgaactttgttgc
<i>STX2</i>	ggaagaatgatgatggagac	agaaagaatgatgctgtggt
<i>STX3</i>	tgctatcgacaacacggctt	ctggaatcgggtcagagaga
<i>STX4</i>	tgagctgcacgacatattca	tgtgcgacattatccaacca
<i>STX6</i>	ggtacagaaagcagtcacac	tcatcaaggctccttagatcc
<i>STX7</i>	aacacctcaagattcactg	gttgtgaactctgccactaag
<i>STX8</i>	aagcttaccgtgacaatcag	aaggatgccagaagtagctc
<i>STX12</i>	atgagccagctaggaactaag	gttcctctgaagtctctgct
<i>STX16</i>	cagcttagatccagaagcag	ctgagtgatctctgggtagtt
<i>STX17</i>	gtccgaaaggatgacctagta	agtcaggtatctgtgcaag
<i>SNAP23</i>	ggacatgagagagacagagaa	gcttgctgttagatactac
<i>SNAP29</i>	agaacaggaagcaaagtacc	ctgtcgatctctggtgatag
<i>Rab1</i>	gttactctgattggcgact	catggctcctctgtaataa
<i>Rab3</i>	cggatcagaactcgcactac	agcttgatcctctgtcgt
<i>Rab5</i>	atacagctggtcaagaacga	ttaggacttgcttgcctct
<i>Rab6</i>	tagcctattcccagttaca	cacttctcttctgtctgac
<i>Rab8</i>	atcacaacggcctactacag	ccttggaacttgctcttg
<i>Rab11</i>	gagctgtaggtgccttattg	gctcttcttctctgtagg
<i>VAMP3</i>	aatcgaagactcagcagac	cagagagctctggtctcttt
<i>VAMP7</i>	cgagttctcaagtgtcttagc	agcaagatttctgctggtag
<i>VAMP8</i>	gagtgaggaggagtaagaat	acaatcacgcagataaggac
<i>18S rRNA</i>	aaccctgtgaaccctatt	ccatccaatcggtagtagcg
UAP	caggctccagtttttttttttgc	
AP	caggctccagttttttttttt	

Fig 1

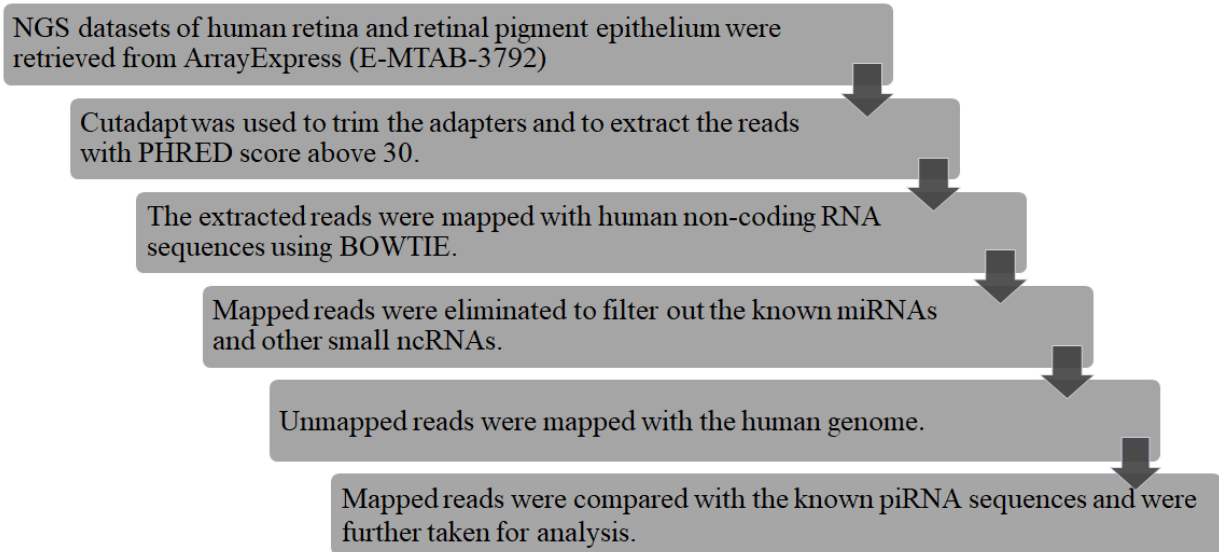


Fig 2

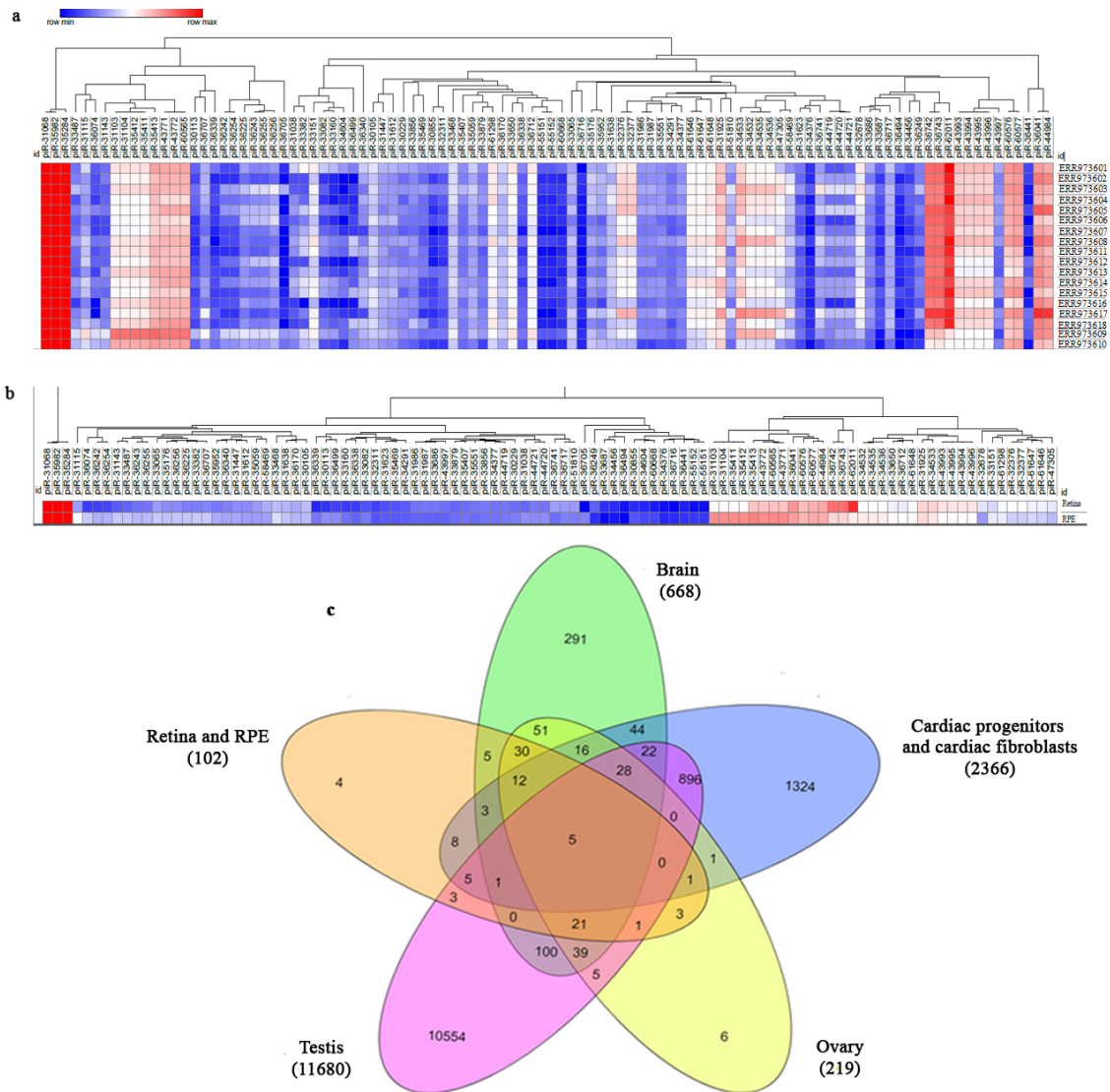
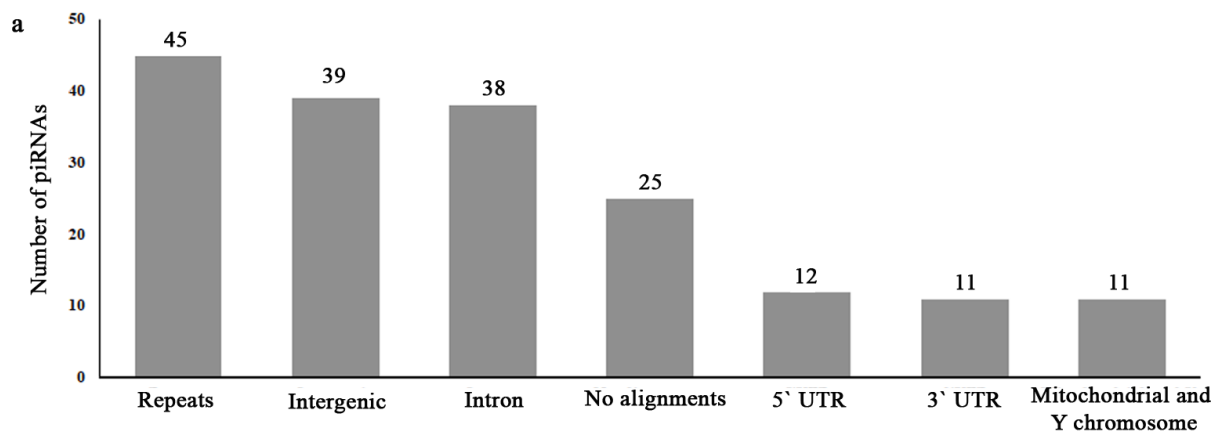


Fig 3



b

piRNA bank ID	Sequence	Gene	Intron	Intergenic	5'UTR	3'UTR	Repeat
piR-31068	agcattggtggttcagtggtagaattctcgc	Vac14	lies within the intron	-	-	-	L1PA5/LINE/L1 and tRNAs Gly
piR-35411	gccccgctagctcagtcggtagagcatgag	NBPF10	lies within the intron	intergenic	-	-	tRNA Lys
piR-36742	gttccgtagttagtggtcaccagttcgc	-	-	intergenic	-	-	tRNA Val
piR-60576	ttccgtagttagtggttatcacgttcgc	-	-	intergenic	-	-	tRNA Val
piR-62011	tttgcaatgtagaactcacactggtgaggt	MIR182	-	-	-	3'UTR of miR 182	-
piR-31104	agccccgctagctcagtcggtagagcatgaga	-	-	-	-	-	tRNA Lys
piR-31925	attggtggttcagtggtagaattctcgcctg	VAC14	lies within the intron	intergenic	-	-	tRNA Gly
piR-35982	ggcattggtggttcagtggtagaattctcgc	VAC14, COLQ	lies within the intron	intergenic	-	-	tRNA Gly
piR-43993	tccgtagttagtggttatcacgttcgcct		-	intergenic	-	-	tRNA Val
piR-60565	ttccctggtggtctagtggttagattcggc	NBPF10, PLCH1	lies within the intron	Intergenic	-	-	tRNA Glu

Fig 4

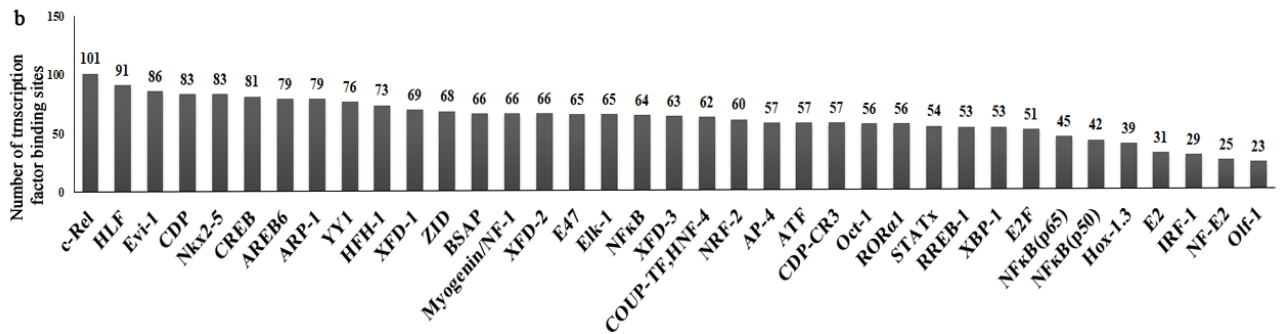
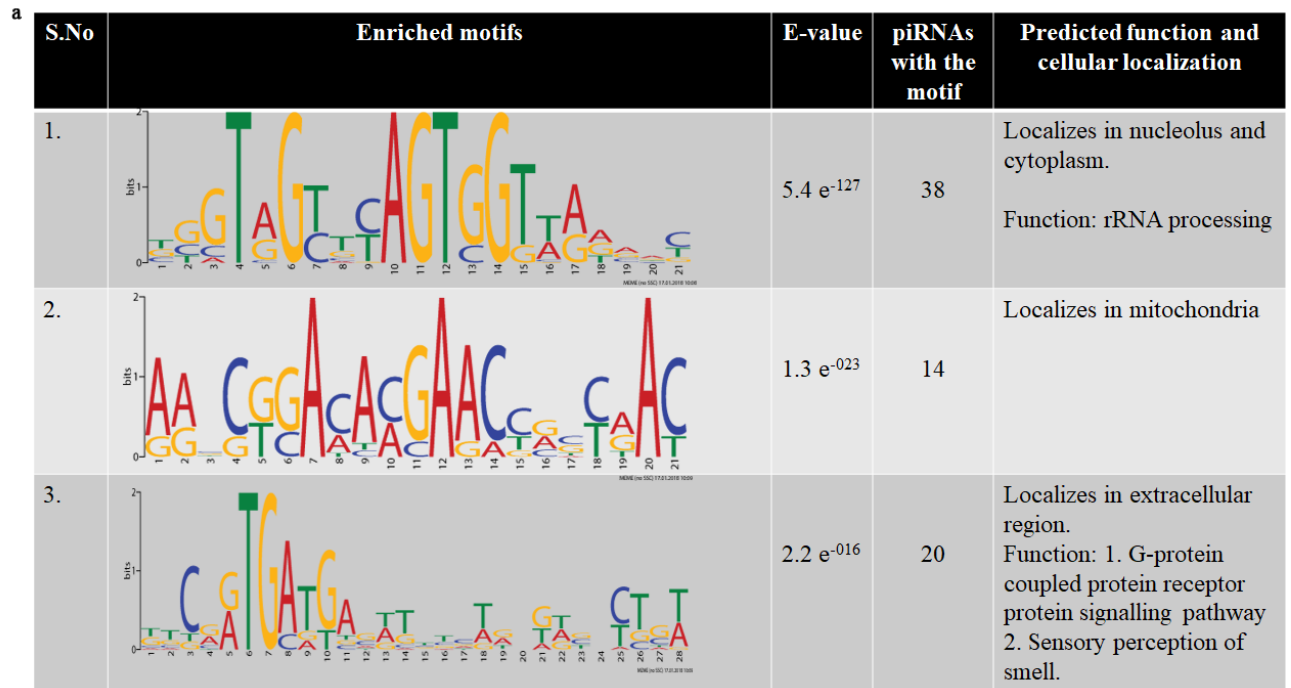


Fig 5

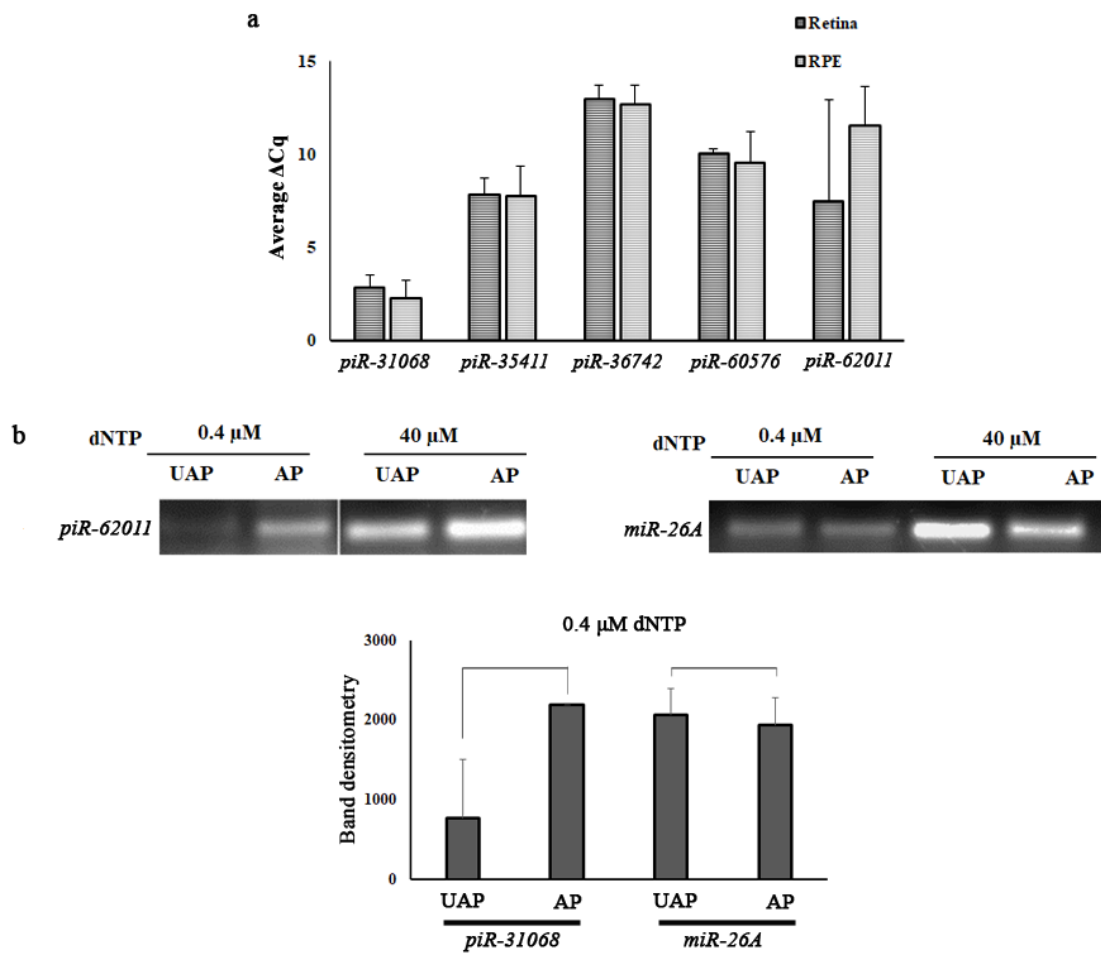


Fig 6

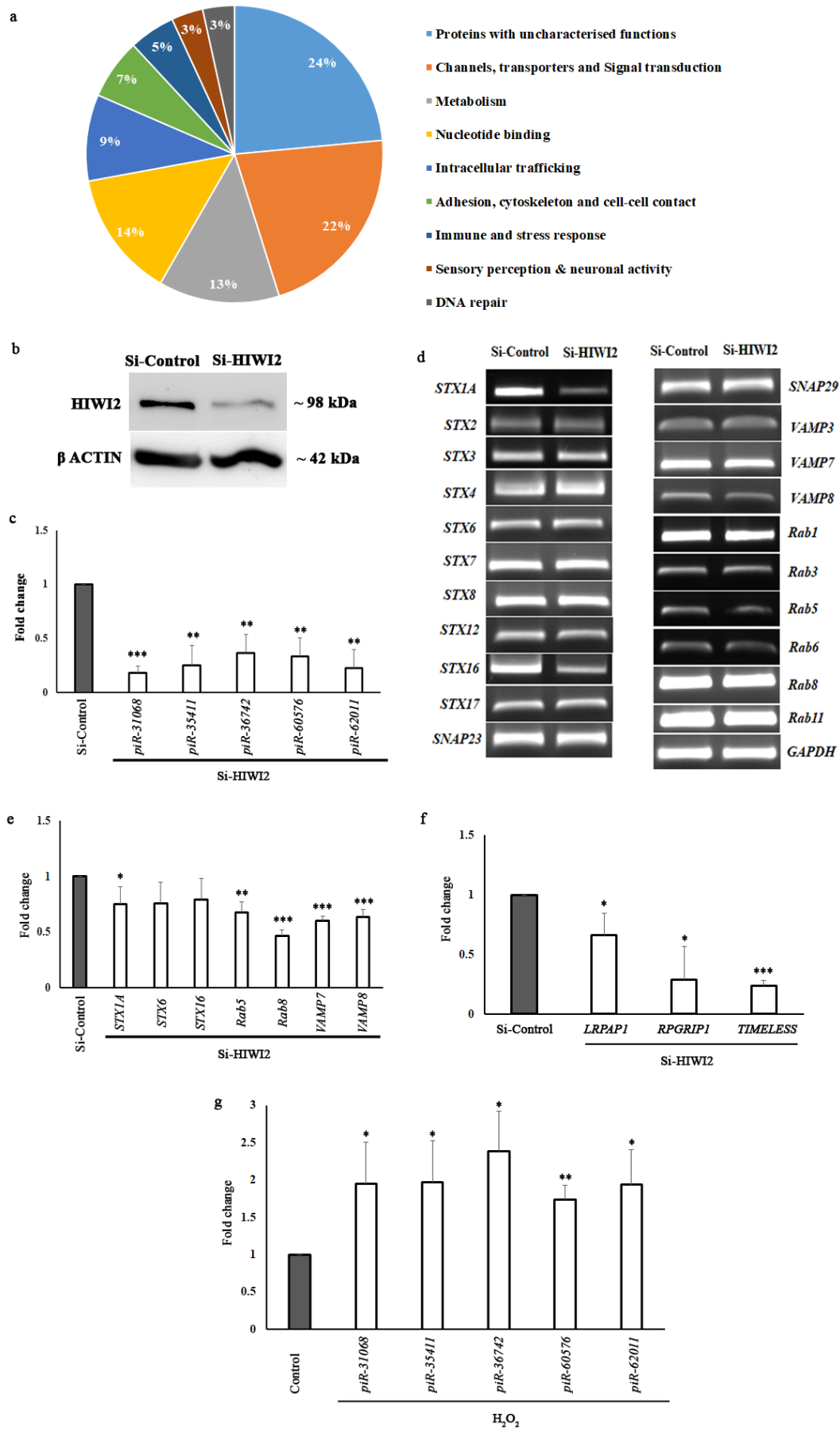


Fig. 8

